

Contents lists available at ScienceDirect

Fuel

journal homepage: www.elsevier.com/locate/fuel



Full Length Article

Clean co-combustion of glycerol and methanol blends using a novel fuel-flexible injector

Timothy Hall, Derek Williams, S M Rafiul Islam, Ishaan Patel, Caleb Chakmakjian, Lulin Jiang *

Department of Mechanical Engineering, Baylor University, Waco, TX 76798, USA



Keywords: Swirl Burst (SB) injector Lean-premixed combustion Glycerol/methanol blends High viscosity Near-zero emissions

ABSTRACT

This study explores combustion of highly oxygenated fuel blends (glycerol/methanol, G/M) to mitigate carbon footprint using a novel fuel injector, called Swirl Burst (SB) injector. The recently developed SB injector yields fine droplets immediately rather than a breaking jet/film of conventional injectors. The advanced atomization resulted in ultra-clean combustion with high fuel flexibility even for viscous oils without fuel preheating. The present work investigates the effects of fuel composition and the atomizing air to liquid mass ratio (ALR) across the injector on the global combustion characteristics of G/M blends without fuel preheating in an uninsulated lab-scale combustor. Results show that the SB injection resulted in mainly clean lean-premixed and near complete combustion for the G/M mixes of 50/50, 60/40 and 70/30 by power with near-zero emissions of CO and NOx. Increase in ALR resulted in more radially distributed flames with slightly reduced flame lift-off height, with ultra-clean and near complete combustion for all the ALRs for the 50/50 and 70/30 blends. Clean and efficient G/M combustion without fuel preheating achieved by the fuel-flexible SB injection signifies the potential to combust crude glycerol — the largest oxygenated byproduct of biodiesel production — to enable biofuel cost effectiveness with near-zero emissions.

1. Introduction

In recent years, near-zero/net-zero-emission and efficient combustion and biofuel applications are urged by the changing climate due to the aggravating global warming. Biodiesel has become an emerging alternative fuel because of its closed carbon cycle and similar fuel properties to conventional diesel. In the European Union (EU), biodiesel production increased from 6.129 millions of tons to 14.11 millions of tons over the year 2007-2018 [1,2]. To create this fuel, highly viscous source oils go through the costly trans-esterification process [3] to form the biodiesel with "drop-in" i.e., similar properties of conventional diesel to be adapted into the existing combustion systems [4]. These systems utilize conventional fuel injectors with a high sensitivity to even a slight variation in fuel properties [5,6]. In addition, the transesterification process creates large surplus of crude glycerol as a waste byproduct, though the crude glycerol can be refined in another expensive process to be used in various food and pharmaceutical products [4]. Cost related to coping with the abundant waste renders the biodiesel production less cost effective, hence limiting its broad application for

decarbonization. On the other hand, the waste crude glycerol can become an extremely low-cost potential fuel [7-9]. Glycerol has a moderate heating value and a high oxygen (O_2) content, and thus, has the potential to be burned as biofuel to mitigate carbon footprint for power generation [4,6,10,11]. However, the high ignition temperature and high viscosity of glycerol and the low-viscosity tolerance of conventional injectors have made it difficult to burn [4,12,13].

Clean and complete combustion of liquid fuels is not only determined by its chemical composition (such as a closed-carbon cycle of biofuels) but also by the complicated physicochemical process of spray combustion [4]. Effective atomization results in fine sprays that evaporate fast, leading to homogenous mixing of fuel vapor and air and thus the clean premixed combustion of liquid fuels with near-zero emissions or netzero emissions when fuels are biobased with closed carbon cycle. Unfortunately, conventional airblast (AB) and pressure swirl (PS) injectors, widely used in gas turbines and other industrial burners generate a liquid jet core/film first that gradually disintegrates into ligaments and ultimately droplets even for low-viscosity water [4,14–16]. Moreover, the jet-breaking atomization is highly sensitive to slight fuel property variations. High viscosity further suppresses the atomization capability

E-mail address: lulin_jiang@baylor.edu (L. Jiang).

^{*} Corresponding author.

Fuel 371 (2024) 132125

Nomer	nclature
CO	carbon monoxide
NO_X	nitrogen oxides
SB	swirl burst
VO	vegetable oil
H	the height between the injector exit and the internal
	liquid tube tip
D	the inside diameter of the internal liquid tube tip
AA	atomizing air
PA	primary air
d_h	hub diameter
d_t	tip diameter
α	angle of swirl (swirl vane angle)
ISN	injector swirl number
SN	swirl number for the combustion swirl of the gas turbine
	combustor
ALR	atomizing air to liquid mass ratio
LPM	lean premixed
G/M	glycerol/methanol

T. Hall et al.

and elongates the atomization process, resulting in ligaments and large droplets [15]. These large ligaments/droplets of viscous fuels burn incompletely and/or in diffusion mode, yielding high pollutant emissions such as soot, toxic carbon monoxide (CO), nitrogen oxides (NOX), and unburned hydrocarbons [4]. For instance, alternative jet fuel C-3 with only 3x higher viscosity than diesel resulted in the poorest ignition and high pollutant emissions compared to other jet fuels by using conventional AB injector [17]. As high-viscosity fuels burn incompletely using the conventional injectors, more fuel mass must be burned to achieve the same heat output compared to conventional low-viscosity fuels such as diesel, or more energy will be needed to preheat the fuels to reduce the viscosity [4]. This effect is further compounded in glycerol combustion because of its relatively low heating value, 15.8 MJ/kg, which is half that of biodiesel [4,7,12,13]. The high viscosity and relatively low energy density signify that novel fine atomization concept with high-viscosity tolerance and/or blending glycerol with fuels with higher heating values are necessitated to enable glycerol as a potential clean renewable fuel and achieve heat output comparable to conventional fuels via co-combustion of glycerol-based blends [4].

In the last two decades, Gañán-Calvo first developed flow-blurring (FB) atomizer which can generate 5–50 times greater surface area than an AB atomizer, via using a novel primary atomization mechanism by bubble bursting that is fundamentally distinct from the typical AB/PS

jet/film breaking [18]. In FB, at a unique simple internal geometry, a small quantity of the atomizing air (AA) that passes through an annular channel around the center liquid channel penetrates into the liquid fuel and rapidly forms bubbles at the inner liquid tube tip [18]. These bubbles burst due to a large pressure drop while leaving the atomizer exit, defined as the primary atomization, shattering the surrounding liquid into fine spray immediately at the injector exit [19], rather than a typical AB/PS jet core/film. The remaining larger portion of AA directly leaves the injector exit and leads to the secondary atomization of liquid by shear layer instabilities developed at the interface of the liquid parts and the high-velocity air [20]. FB can generate ultra-fine sprays for various liquids [15] ranging from low-viscosity water, to high-viscosity alternative jet fuel C-3 [21], and even extremely viscous pure glycerol [22] without fuel preheating. Simmons et al. observed that for atomizing air to liquid mass ratio (ALR) of 2.5, with the injector exit diameter (D) of 1.5 mm, FB can generate more uniform final water droplets with the Sauter Mean Diameter (SMD) of 5–15 μ m, compared to SMD of 5–25 μ m for the AB injector with the injector orifice D of 0.15 mm at >2 cm downstream the exit [15]. Oavi et al. found that FB injector, with the injector D of 1.5 mm, generated fine droplets with the size of 90 % < 45-70 µm for the ALRs of 1.00 to 2.5 respectively within 6 mm downstream of the injector exit for the viscous alternative jet fuel C-3 (blends of farnesane and JP-5) [21]. Even for the high-viscosity glycerol (~>200x more viscous than diesel), FB injector generates thin ligaments and fine droplets with the thickness or diameter $<\!40~\mu m$ at 0--2~mmlocated at the downstream direction from the injector exit [22]. Thus, it has enabled ultra-clean, complete, and lean-premixed combustion of distinct fuels including diesel, biodiesel, straight vegetable oil and straight glycerol [10,23–25]. However, relatively larger droplets occur at the FB injector spray periphery [26]. Also, while atomizing the extremely viscous pure glycerol by using an FB atomizer, the thin ligaments undergo secondary atomization by shear layer instabilities [22], yielding a longer atomization completion length compared to the lower viscosity liquids. Hence, though complete, ultra-clean and leanpremixed combustion was even achieved for the non-preheated straight glycerol by FB injection, the flame lift-off height was increased compared to the lower-viscosity fuels, compromising its flame stability [19].

To further improve the secondary atomization with a wide range of viscosity tolerance, our group recently developed a novel Swirl Burst (SB) injector [27,28]. The SB injector integrates the bubble-bursting primary atomization mechanism of the FB and novel swirling channels on the chamfered exit to guide the AA to leave the injector exit in a swirling pattern (as a combined radial and axial swirl) to rigorously enhance the interaction between the liquid parts and the swirling AA, resulting in more robust secondary breakup. Fig. 1 (a)-(c) show the

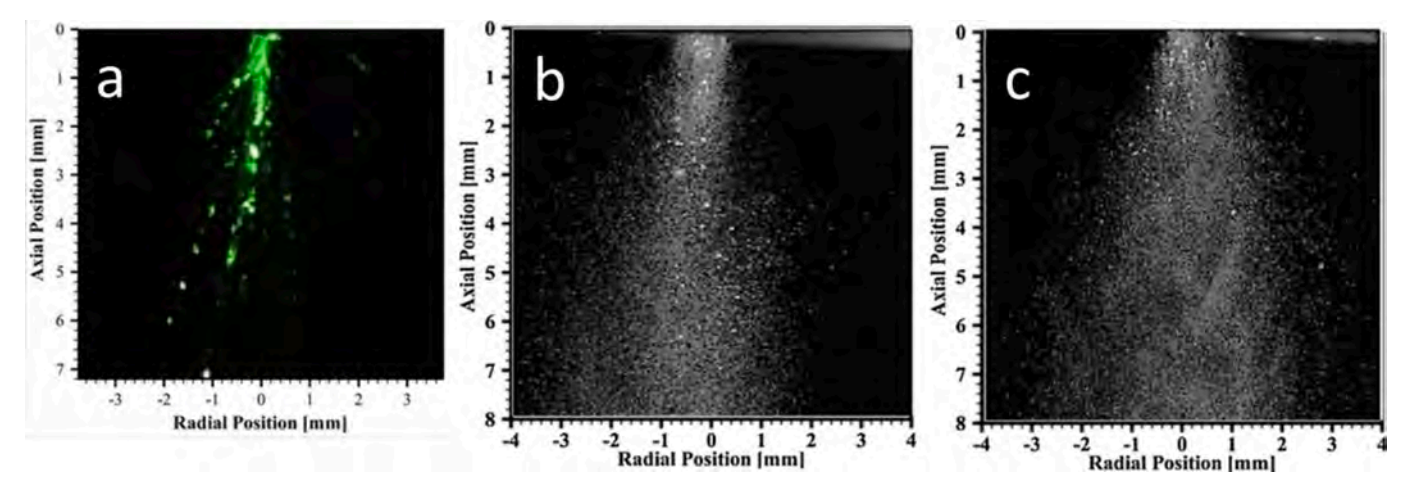


Fig. 1. Comparison of water spray images from (a) AB injector [26] (b) FB injector and (c) SB injector [27].

water spray images by AB, FB and SB injectors respectively [26,27]. Compared to the AB jet core, both FB and SB injectors generate fine droplets at the injector immediate exit with more diverged spray angle for the SB injection. Advanced laser diagnostics in the injector near field also quantitatively substantiated that the SB injector generates finer droplets at the spray periphery with more uniform droplet size distribution and halved atomization completion length than that of an FB injector [27-29]. Thus, the SB injector enabled lean-premixed and complete combustion with ultra-low emissions for fuels including diesel, biodiesel, viscous straight vegetable oil (VO), and straight algae oil (AO), without fuel preheating nor hardware modification [4,19,20]. The VO and AO are approximately 15 times or 16 times more viscous than diesel [4,19,20]. The flame lift-off height of the straight VO sprays formed by the SB injection was also shortened compared to that of the FB atomizer, enhancing the spray combustion stability, as over-lifted flames are subjective to blow out [4,19]. A previous version of the novel twophase injector with high-viscosity tolerance but a longer atomization length [21,27,29] also resulted in clean and complete combustion of straight glycerol (>200 times more viscous than diesel) without fuel preheating, though an insulation layer was used to minimize heat loss [4,10]. This novel injector design transforms the conventional jetbreaking atomization into ultra-fast and fine atomization with high fuel flexibility [4]. Compared to a sooty flame with droplets incompletely burned by jet-breaking conventional injection, the SB injector thereby not only enables complete and lean-premixed combustion of low-viscosity liquid fuels, but also enables the ultra-clean and efficient combustion of highly viscous waste glycerol, transforming it into a potential cost-effective biofuel and making the biodiesel production more economically friendly.

On the other hand, crude glycerol formed as a biodiesel byproduct contains a major impurity in the form of methanol [4,6,11,30,31]. Methanol is an extremely low viscosity liquid that is used in excess during the trans-esterification process to help convert reactants to biodiesel [4,7]. Besides, methanol has high octane number that could prevent engine from knocking and reduce greenhouse gas emissions [32]. While it can be removed and reused in the trans-esterification process, methanol is typically left with the crude glycerol and disposed of because it is easier and cheaper to use a pure supply [4,7,31]. Also, energy consumption for extracting methanol from biodiesel production is almost 48 % of total energy consumption of biodiesel production [33]; hence, it is a highly energy expensive process. Compared to glycerol, glycerol/methanol blends, the main components of crude glycerol, can achieve a significantly lower viscosity that is comparable to that of diesel, easing the fuel atomization when using it as a fuel source [4,7,34]. Crude glycerol from the transesterification process of biodiesel production contains 60-70 % glycerol and 23.4-37.5 % methanol by weight [6]. Thus, the current study examines glycerol and methanol blends with the composition representing the crude glycerol to avoid the need for possible further refinement of crude glycerol, which could enhance its cost-effectiveness as a potential waste-based biofuel to produce renewable energy [4]. Furthermore, methanol blended with glycerol helps to avoid heat loss, lower the fuel viscosity, and benefit carbon mitigation as an oxygenated fuel [4,7].

The combustion performance of glycerol/methanol (G/M) blends is rarely investigated. Agwu et al. [7] investigated the G/M flame characteristics (luminosity, stability etc.) but not the emissions using a conventional pressure swirl injector that is based on jet/film breaking atomization, which generated sooty orange flames. Jin et al. showed that, for Spark Ignition Engine (SIE), by adding 5 % glycerol with methanol by volume can increase the thermal efficiency from 38.3 % to 43.1 %, while NOx emissions and soot in the exhaust gas remain unchanged compared to the 100% methanol fuel [35]. Oliveria et al. combusted glycerol by chemical looping combustion process and achieved 90 % combustion efficiency at oxygen to fuel molar ratio of 7, water/glycerol ratio of 0.75 and with reactor temperature of 1023 K [36]. In the current study, the swirl burst (SB) injector, with the

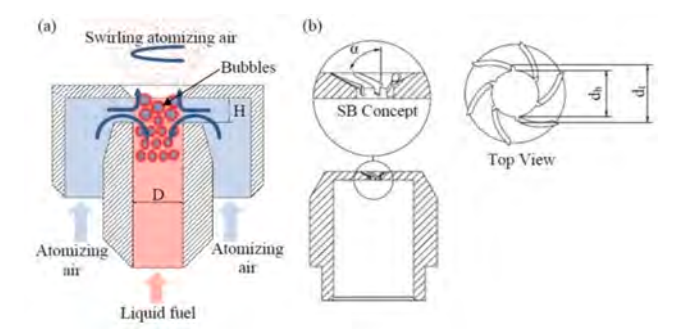


Fig. 2. (a) working principle of the SB injector (b) SB concept [4,19,20].

preliminary results that proved high viscosity tolerance [19,20], is expected to achieve complete, clean, and stable combustion of glycerol-methanol blends without fuel preheating [4]. The objective of this experiment is to discover the impacts of fuel composition of glycerol and methanol and the atomizing air to liquid mass ratios (ALR) on the global combustion characteristics using the novel SB injector in a lab-scale swirl-stabilized gas turbine combustor [4]. The flame features of interest include visual flame images, product gas temperatures, and emissions (CO and NO_X) to assess global combustion completeness, cleanness, and flame stability [4]. The novelty of the current study is thus focused on potentially enabling direct use of crude glycerol for waste to energy with minimal processing by achieving clean and nearly complete combustion of different non-preheated high-viscosity glycerol and methanol blends representing crude glycerol using the SB injector.

2. Experimental setup

2.1. Swirl burst injector

The working principle and concept of the swirl burst injector are illustrated in Fig. 2, which are detailed in Ref. [4,19,20,27,28]. The SB injector has two stages of atomization [4]. The first stage occurs while the AA in the annulus channel surrounding the liquid tube bifurcates and incurs the backflow of a small amount of AA into the liquid tube tip, when the geometric conditions are met: (1) *D* of the internal liquid tube is equal to that of the injector exit; (2) the gap, H, between the liquid tube tip and the injector exit is $\leq 1/4D$ [4]. The AA backflow rapidly forms a bubble zone with pockets of air enclosed by liquid at the liquid tube tip [4]. The bubbles expand and burst, causing the surrounding liquid to shatter into fine droplets while exiting the injector, due to a quick pressure drop [4]. The remaining AA exits the chamfered injector orifice through small grooves in a swirling motion [4]. This causes increased shearing between the liquid and AA around it, further breaking down the liquid into smaller droplets [4,27,28]. The swirling grooves in the orifice are defined by three parameters called the hub diameter (d_h) , tip diameter (d_t) , and swirl vane angle (α) [4]. The hub and tip diameter describe the volume of air/fuel mixture that passes through the grooves, while the swirl angle describes the angle at which the liquid (fuel mixture) is swirled as it exits the injector [4]. The swirl burst injector exit orifice is defined using a non-dimensional injector swirl number (ISN) as in Eq. (1) [4,27,28,37]. It is a non-dimensional number representing the axial flux of swirl momentum divided by the axial flux of axial momentum times equivalent nozzle radius [4,37]. The current study uses the SB injector with D of 1.5 mm, H of 0.375 mm, and ISN of 2.4 [4].

$$ISN = \frac{2}{3} \times \frac{1 - (d_h/d_t)^3}{1 - (d_h/d_t)^2} \times tan\alpha$$
 (1)

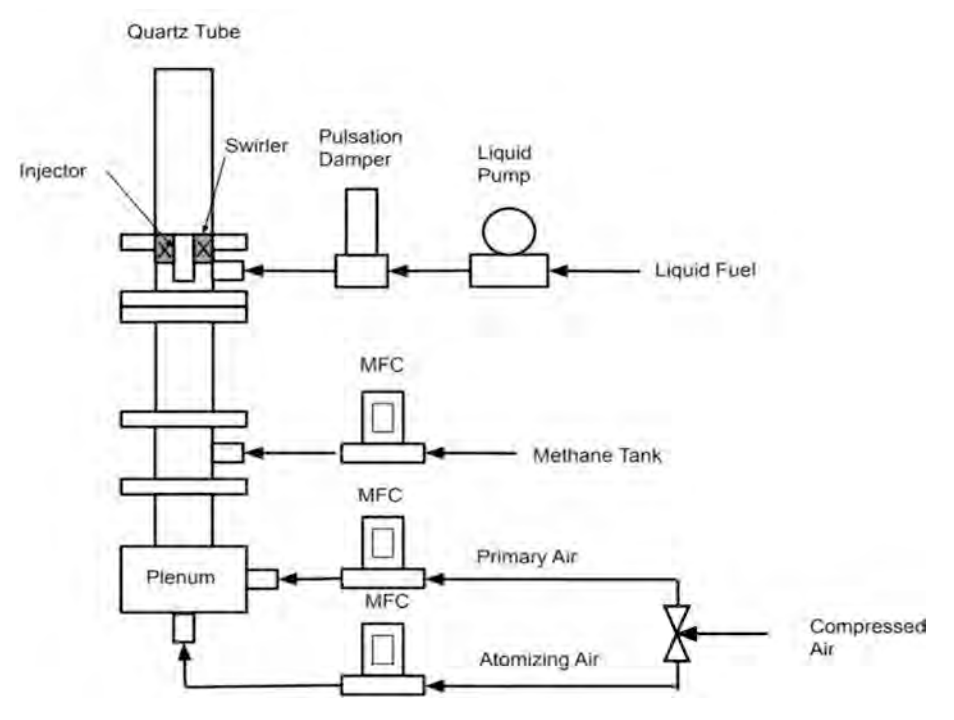


Fig. 3. Schematic of the experimental set-up [4].

2.2. Combustion system

Fig. 3 shows the experimental setup of the lab-scale swirl-stabilized gas turbine combustion system [4]. The in-house compressed air, after passing through water traps and filters to ensure clean air, is split into two lines [4]. The first line is the primary air for combustion [4]. The second line, atomizing air, connects to the SB fuel injector that is installed in the center of the downstream dump plane [4]. Both lines are controlled with mass flow controllers (MFC) [4]. The mass flow controllers are both Alicat MC-series controllers with a range of 0-100 SLPM for the atomizing air and a range of 0–250 SLPM for the primary air [4]. Both mass flow controllers have an uncertainty of 0.8 % of the reading ± 0.2 % of the full range [4]. The primary air flows into a mixing chamber filled partially with marbles to ensure a laminar and even flow [4]. Methane flows into the mixing chamber from a compressed natural gas tank [4]. The flow is controlled with another Alicat MC-series controller with a range of 0-50 SLPM [4]. For air and methane flow control, all the MFCs use standard conditions and the set value of the standard condition is 25°C temperature and 1 atm pressure. Also, the ambient temperature of the laboratory is 22°C throughout the experiment. To ensure the repeatability of the experiment, preliminary test is conducted by taking emission and temperature data at the combustor exit to ensure the injector and combustor system is function well without leakage. In the mixing chamber, methane is premixed with the primary air which then enters a quartz combustor tube through an axial swirler with a swirl number (SN) of ~ 0.75 [4]. The quartz tube is 45 cm long and 7.62 cm wide [4]. The methane/air flame is used to preheat the chamber before switching the gaseous fuel to fully liquid fuel blends [4]. The liquid fuel blend is delivered through a pulsation damper by a peristaltic pump [4]. The peristaltic pump is a Cole-Parmer Masterflex L/S (EW-77921-75) with a range of 0-88 mLPM and an uncertainty of ± 0.1 % of the reading [4]. The liquid fuel then enters the fuel injector before entering the quartz combustor as a fine spray [4]. The fuel blends are atomized using the swirl burst injector with the ISN of 2.4 [4].

2.3. Experimental conditions

The fuel blends of glycerol and methanol in this experiment are 50/

Table 1Selected properties of the relevant fuels [4,7,10,12,13,38–40].

Property	Diesel	Methanol	Glycerol
Approximate chemical formula	C _{11.125} H _{19.992}	CH ₄ O	$C_3H_8O_3$
Lower Heating Value, LHV (MJ/kg)	44.6	19.9	15.8
Density at 25 °C (kg/m ³)	834.0	791	1260
Kinematic viscosity at 25 °C (mm ² /s)	3.88	0.59	965.8
Auto-ignition temperature (°C)	260	464	370
Vaporization temperature (°C)	160-370	64.7	290
Heat of vaporization (kJ/kg)	250	726.1	662
Stoichiometric air/fuel ratio (mol/mol)	16.12	7.14	16.66

Table 2
The experimental conditions and fuel properties of the tested fuel blends [4].

-				
Property		50/50	60/40	70/30
Percent heat output	Glycerol	50 %	60 %	70 %
	Methanol	50 %	40 %	30 %
Mass flow rate (g/min)	Glycerol	13.29	15.95	18.61
	Methanol	10.53	8.44	6.33
	Total	23.84	24.39	24.94
Volume flow rate (mLpm)	Glycerol	10.55	12.66	14.77
	Methanol	13.34	10.67	8.01
	Total	23.89	23.33	22.77
Atomizing air flow rate (SLPM)		56.09	57.37	58.66
Primary air flow rate (SLPM)		87.96	86.99	86.02
Density at 25 °C (kg/m ³)		998.09	1045.46	1095.15
Kinematic viscosity (mm ² /s) at 25 °C		4.16	8.02	18.02

50, 60/40, and 70/30 of glycerol/methanol by percent heat output at a constant theoretic heat release rate (HRR) of 7 kW and a constant equivalence ratio (ER) of 0.75 [4]. Table 1 provides physical properties of glycerol and methanol compared to conventional diesel fuel [4]. The experimental conditions and the properties of the fuel mixes are listed in Table 2 [4]. The viscosity calculations for the fuel blends in Table 2 are calculated with the method detailed by O. Agwu et al in [4,7]. The fuel blends are fed into the twin-fluid SB injector at ALR of 1.5, 2.0, 2.5, and 3.0 for the spray combustion in the 7-kW swirl stabilized gas turbine

Fuel 371 (2024) 132125

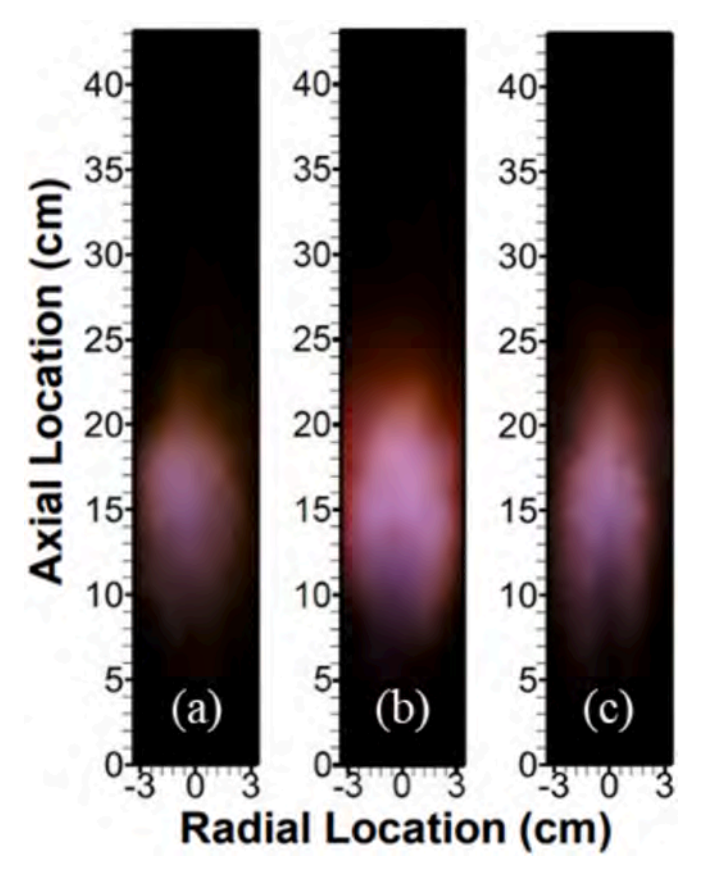


Fig. 4. Flame images of glycerol/methanol fuel mixes by power of (a) 50/50 (b) 60/40 and (c) 70/30 at the constant ALR of 3 and constant HRR of 7 kW [4].

combustor [4]. The combustion of the three fuel blends also remains at the constant equivalence ratio of 0.75 [4]. The combustion products including NOx, CO, carbon dioxide (CO₂) and O₂ are measured using an ENERAC (700 series) emission gas analyzer [4]. The analyzer can detect NOx in dual range mode of the low range 0-50/150 ppm and 0-1500 ppm with a resolution of 0.1 ppm and an uncertainty of $<\pm1\%$ of measurement [4]. For CO, the measurement range is low range 0-50/ 150 ppm and 0-2000 ppm with a resolution of 0.1 ppm, an uncertainty of ± 1 –2 % of measurement [4]. The O₂ sensor has a range of 0–25 % with 0.1 % resolution, an uncertainty of ± 0.2 % of the reading [4]. The catalytic sensor that detects the combustibles has a range of 0-5 % with an uncertainty of ± 2 % [4]. The temperature of the exhaust gas is measured with a type K thermocouple plugged into the emissions analyzer with a range of 0-1100 degrees Celsius and an uncertainty of 2 degrees Fahrenheit [4]. The thermocouple is placed inside of a thin hollow probe that also collects a continuous sampling of exhaust gas for the emissions analyzer [4]. The emissions are collected at the combustor exit, i.e., 1 in. upstream the quartz opening, to assess the combustion completeness and cleanness [4].

3. Results and discussion

3.1. Effect of fuel blends on global combustion characteristics

3.1.1. Global flame characteristics

This study first investigates the effect of various fuel mixtures [4]. The largest apparent difference is the kinematic viscosity of each mixture shown in Table 2 [4]. The density for 70/30 G/M increases up to 10 % from the density of G/M 50/50. The viscosity varies from 4.16 mm^2/s for 50/50 G/M, which is only slightly more viscous than diesel in Table 1, to 18.02 mm^2/s for 70/30 G/M, i.e., >5x more viscous than diesel [4]. Flow rates are similar at the constant HRR of 7 kW as

illustrated in Table 2. Visual flame images are taken to qualitatively analyze the cleanness and structure of the flame [4]. Flame lift-off heights and flame lengths are estimated [4]. Flame color indicate flame cleanness related to the chemiluminescence [4,12,32]. For example, blue flames represent chemiluminescence of complete combustion of CH* [24]. The flame images of G/M fuel blends with a ratio of 50/50, 60/40 and 70/30 by HRR are illustrated in Fig. 4. In all the three cases the equivalence ratio and the ALR are maintained at 0.75 and 3.0 respectively. Fuel atomization, fuel pre-vaporization, and fuel-air mixing occurs in the dark area near the injector exit and upstream the flame front, indicating that the mainly lean-premixed (LPM) combustion has achieved for all the three fuel blends [4]. The main blue color in all the flames qualitatively signifies that all the fuel blends are combusted cleanly. The overall physical flame structure is similar for all the flames, signifying the high fuel flexibility of the novel SB injection regardless of the distinct variation of the fuel viscosity [4]. The visual flame begins near the axial location of y = 10 cm (with y = 0 for the dump plane) in each fuel mix [4]. However, the 50/50 mixture creates a slightly more compact and faint flame than the other two mixtures [4]. The 50/50 mixture's visual flame is located slightly further downstream than the other two mixes at y = 11 cm [4]. It ends at y = 23 cm, while the other two end further downstream at 24-cm [4]. The flame lengths are \sim 12 cm $(y = \sim 11-23 \text{ cm})$, 15 cm $(y = \sim 9-24 \text{ cm})$ and 15 cm $(y = \sim 9-24 \text{ cm})$ respectively for the 50/50, 60/40 and 70/30 glycerol/methanol (G/M) mixes [4]. The slight variation is possibly due to (1) the higher viscosity of the 60/40 and 70/30 fuel mixtures causing large droplets to penetrate deeper into the reaction zone more often which increases the residence time of combustion, thus a slightly elongated flames, and (2) more glycerol for the 60/40 and 70/30 resulting in slower vaporization, ignition, and thus slower oxidation due to the high vaporization and auto-ignition temperature of glycerol [4]. The slightly increased flame lift-off height of the G/M 50/50 is likely due to the higher AA flow rate causing a higher injection velocity for the fuel mixture [4].

From the flame images in Fig. 4, it is observed that the flame area of 50/50 G/M is most compact. The 60/40 G/M is with the largest flame area with the longest and widest flame among the three cases. The 70/30 G/M flame has a slightly shorter length than 60/40 G/M flame but the narrowest flame among the three. The flame structure variation is possibly attributed to the combined effects of (1) the fuel blend viscosity; (2) the composition of the glycerol component that has high evaporation and ignition temperatures; (3) the fuel injection velocity determined by the AA flow rate. Among the three blends, 50/50 G/M is the least viscous with the lowest AA thus lowest injection/droplet velocity, and the least glycerol amount as shown in Tables 1 and 2. The lowest viscosity could result in the finest droplets, with the least glycerol amount, which lead to the most rapid fuel evaporation, ignition and thus the fastest oxidation rate, yielding the most compact flame. The lowest injection velocity further enhances the fuel residence time to ensure more complete combustion as substantiated in the later combustion efficiency estimate. The more viscous 60/40 G/M may result in larger droplets than those of 50/50 G/M, plus with more glycerol component, the evaporation rate and thus the subsequent ignition and fuel oxidation rate are all slower than those of the 50/50 G/M droplets, resulting in an elongated flame zone with less completed combustion. The in-between injection velocity ensures more residence time of most of the fuel in the combustor than the 70/30 G/M flame, with less glycerol, yielding the longest flame among the three. The largest width of the 60/40 G/M flame also suggests that though the viscosity is higher than that of the 50/50 G/M, droplets are still fine enough to be burned at the near wall zone due to the fine SB atomization. However, for the 70/30 G/M blend, the viscosity is >2x higher than 60/40 G/M, which might generate more larger droplets at the spray periphery. Those large droplets closer to the wall with the highest glycerol component and highest injection velocity undergo incomplete evaporation and combustion, and rapidly escape from the combustor, leading to the lowest reaction rate at the wall and hence the narrowest flame. As the result, it generates the lowest combustor surface

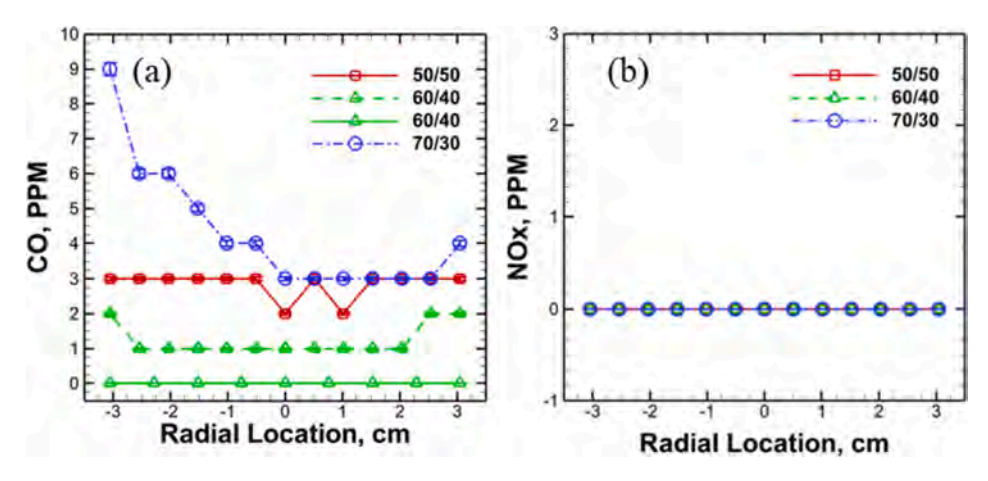


Fig. 5. Radial profiles of (a) CO and (b) NOx emissions at the combustor exit for all the tested fuel mixes [4].

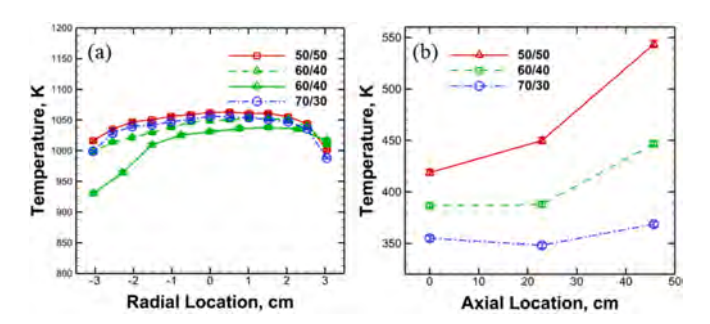


Fig. 6. (a) Radial temperature profile of combustion products (uncorrected) at the combustor exit, and (b) combustor surface temperature [4].

temperature substantiated later in Fig. 6 (b). Compared to the larger fuel drops at the spray periphery, the relatively finer droplets in the combustor center experience slow evaporation, ignition and oxidation, leading to a long flame. The comparable flame length of 70/30 G/M to that of the 60/40 G/M blends again suggests that the sizes of the droplets generated at the combustor center are comparable to those of 60/40 G/ M, though more larger ones at the periphery. This again shows the fine atomization and high-viscosity tolerance of the SB injection. This is consistently validated by the comparable combustion efficiency of the 60/40 G/M and 70/30 G/M blends (90.3 % vs 90 %) in the later section, which also indicates most of fuel is atomized in the center regardless of the discrepancy at the spray periphery and closer to the wall. It is worth mentioning that compared to the mainly lean-premixed G/M flames by the novel SB injector, even at 7 kW for G/M 70/30 (by power), a standard pressure swirl injector resulted in mainly diffusion combustion for G/M 30/70 (by volume) at 6 kW that has less glycerol [4,6]. This suggests the significantly improved SB atomization with considerably finer sprays that evaporated rapidly, mixed more homogeneously with air and burned at premixed mode, even for G/M 70/30, which is \sim 9x more viscous than the G/M 30/70 (by volume) [7] and more difficult-toevaporate glycerol [4]. Note that the representative visual flame images are intended for qualitative information only and flame fluctuation due to turbulence causes variation within the flame [4]. The quantitative data displayed below may be used for a more detailed analysis of fuel combustion [4].

Fig. 5 illustrates the radial profiles of CO and NOx emissions at the combustor exit for each fuel mixture at a constant ALR, equivalence ratio, and HRR [4]. The experiment repeatability is depicted using two experimental data sets of gas temperature and emissions measurements of the 60/40 G/M blends at the combustor exit, shown in Figs. 5 and 6 (a). The discrepancy of 1–2 ppm is acquired for the CO emissions with 0 ppm of NOx concentrations measured for both cases, suggesting the

repeatability. For both tests, the temperature profiles are following similar trend with uncertainty of 5-18 K for the main flame zone, though a higher discrepancy of ~65 K is observed at one side of the combustor zone. This is highly likely due to the uncertainty of the mass flow controllers (MFCs), shown in Section 2.2. The MFCs measure the actual flow rates based on the setpoint. Though the setpoint of both cases are identical (57.37 SLPM and 86.99 SLPM for AA and PA respectively as shown in Table 2), the actual AA and PA flow rates are 56.09 SLPM and 88.06 SLPM respectively for the test 1 (dashed green line in Fig. 5). For test 1, the lower AA flow rate might lead to some slightly larger droplets at the spray periphery. Those larger drops combust at local diffusion mode without full vaporization, resulting in slightly higher local temperature at the near wall zone in Fig. 6 (a), and slightly higher CO concentration consistently shown in Fig. 5(a). The asymmetry is mainly due to the imperfect injector manufacturing that results in asymmetric droplet size distribution on both sides as shown in previous studies [4,27,28]. Regardless of the temperature discrepancy near the wall, the experiment is repeatable with the measurement uncertainties for NOx, CO emissions, and temperature of 0, 1-2 ppm, 5-18 K respectively for the main flame.

All the three fuel mixtures yielded low emissions of CO (<10 ppm) and no NOx emissions indicating ultra-clean combustion [4]. The CO emissions for 50/50 and 60/40 mixes are within the measurement uncertainty [4]. The 70/30 mixture of glycerol/methanol by percent HRR tends to have slightly higher CO emissions mainly close to the combustor wall [4]. This is possibly due to (1) the higher viscosity of the mixture which resulted in larger droplets, especially on the spray periphery [4]. The larger droplets tend to penetrate the reaction zone without complete evaporation, thus burning in diffusion mode and yielding the slightly higher CO emissions; and/or (2) the lower combustion gas temperature thus lower CO oxidation rate closer to wall, as in Fig. 6 due to heat loss of the uninsulated quartz combustor to the surrounding by convection and thermal radiation [4]. NOx is not present for the tested fuel mixes mainly due to the low flame temperature as shown in Fig. 6 [4]. Without any nitrogen content in the fuels, thermal NOx favoring high temperature is mainly from N_2 in air at temperature higher than 1800 K [4,41]. In summary, the global thermal and emission characteristics of the combustion exhaust gases quantitatively suggest clean combustion achieved for all the tested fuel mixes by the SB injection without fuel preheating, regardless of the wide discrepancy in the fuel viscosity and the high evaporation and auto-ignition temperatures of the glycerol component [4].

3.1.2. Combustion efficiency

Combustion completeness is estimated by considering the energy transfer from the combustor as detailed in [4,10]. Low surface temperatures at the outside of the quartz combustor are due to the heat loss via

T. Hall et al. Fuel 371 (2024) 132125

convection and radiation from the combustor surface to the surroundings [4]. To get an accurate assessment of heat loss from the combustor, the gas temperatures measured by the thermocouples are corrected as the thermocouple bead also experiences heat losses through conduction and radiation [4]. Heat loss from the thermocouple bead causes readings to be lower than the true gas temperature [4]. Radiation correction of the gas temperature can be found using Eq. (2) below [4].

$$h_t(T_g - T_t) = \varepsilon_b \sigma(T_t^4 - T_s^4) \tag{2}$$

where T_g is the true gas temperature, T_t is the temperature measured by the thermocouple, T_s is the ambient temperature, σ is the Stefan-Boltzmann constant, $\varepsilon_b = 0.89$ is the type K thermocouple bead emissivity, and finally $h_t = 174 \text{ W/m}^2\text{K}$ is the estimated forced convective heat transfer coefficient over the thermocouple bead [4,19,42]. The difference between the thermocouple reading and the calculated true gas temperature is about 340 K for each of the three mixtures [4]. Solving Eq. (2) for T_g allows a more accurate estimate for the energy released during combustion [4].

To analyze the combustion completeness of each fuel blend, the total energy released during combustion is estimated by adding up the leaving energy carried by exhaust gases using the correct gas temperatures at the combustor exit, and the heat losses from the combustor wall to the surrounding using Eqs. (3)–(5) as below [4].

$$Q_{total} = Q_{gas} + Q_{losses} \tag{3}$$

$$Q_{gas} = m_g C_{P_{oir}} T_g \tag{4}$$

$$Q_{losses} = h_a A_s (T_w - T_{surr}) + \varepsilon_{glass} \sigma A_s (T_w^4 - T_{surr}^4)$$
(5)

where Q_{total} is the total energy released from the combustion process, Q_{gas} denotes energy carried by the leaving combustion gases, calculated in Eq. (4), and Q_{losses} are energy losses from the combustion gases through the combustor outer wall to the surroundings, via convection and thermal radiation, calculated in Eq. (5). m_g is the mass flow rate of the combustion gases, calculated by summing the liquid fuel mass flow rate and the total air mass flow rate [4]. T_g stands for the true gas temperature calculated previously using the measured temperature by the thermocouple in Eq. (2). Specific heat capacity of the combustion product gases, $C_{P_{air}}$, is estimated for the exhaust gas products of gas mixtures: CO2, steam (H2O), O2 and N2, approximating complete combustion for lean conditions at the combustion gas temperature, T_g [4]. The $C_{P_{nir}}$ for each mixture at the average combustion gas temperature is 1.383 kJ/kg K, 1.372 kJ/kg K, and 1.375 kJ/kg K for the 50/50, 60/40, and 70/30 fuel mixtures respectively [4]. The value of $C_{P_{oir}}$ is estimated from the calculated C_P value of exit gas CO_2 , N_2 , O_2 and H_2O [43] at average corrected exit gas temperature T_g . A_s is the combustor surface area, which is equal to 1077.25 cm^2 , σ is the Stefan-Boltzmann's constant, and T_w and T_{surr} are the temperatures of the combustor outer wall surface and the surrounding respectively [4]. Combustor outer wall temperature (T_w) is taken in 3 different sections (1 in. downstream of the dump plane, i.e. the quartz combustor bottom, combustor center, 1 in. upstream from the combustor exit) along the combustor gas flow direction, i.e., the axial direction. ε_{glass} is the emissivity of quartz glass, varies along the length of the combustor as a function of the surface temperature and glass thickness [4]. This value is estimated by using [44]. The emissivity is extrapolated for each fuel mixture at the three surface temperature measurements taken in Fig. 5 (b) [4]. For 50/50 G/ M blend, the estimated emissivity values for the three corresponding temperature and segments of the combustor wall are 0.6782, 0.7032 and 0.7121 from bottom to top. Estimated emissivity for 60/40 blend are 0.7042, 0.7212 and 0.7217, and for 70/30 blend are 0.7272, 0.7336 and 0.7315. These values are used to estimate the heat loss from the outside surface of the quartz glass by thermal radiation in 3 segments of the combustor quartz glass, based on the quartz combustor wall temperature

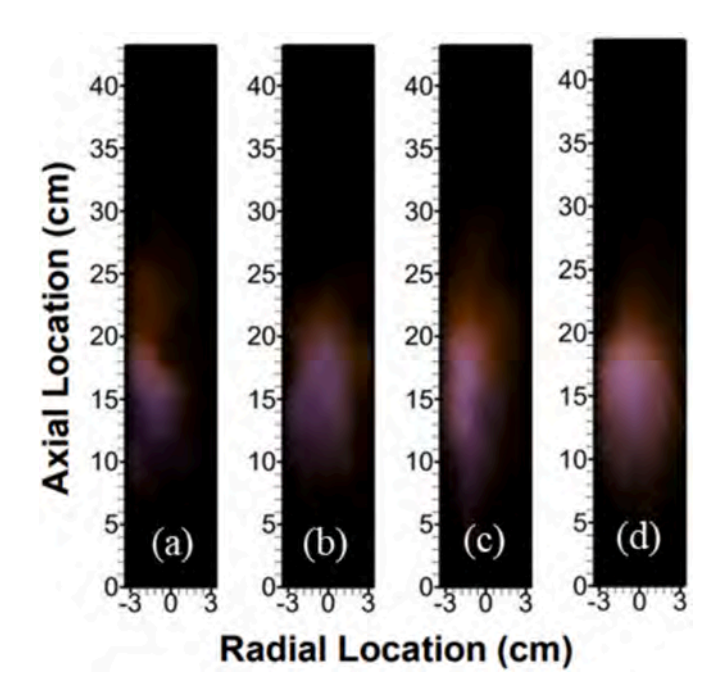


Fig. 7. Flame images for glycerol/methanol (G/M) fuel mixture of 50/50 at ALRs (a) 1.5 (b) 2.0 (c) 2.5 and (d) 3.0 at the constant HRR of 7 kW and equivalence ratio of 0.75 [4].

at bottom, middle and top of the combustor [4]. Natural convective heat transfer co-efficient, h_a is estimated by using the natural convective heat transfer equations [45]. Adding the heat loss through each segment of the combustor outer wall, total heat loss to the surrounding by the combustor wall is estimated.

The released heat of each mixture is estimated to be 6.63 kW, 6.32 kW, and 6.30 kW for the 50/50, 60/40, and 70/30 fuel mixtures, at an ALR of 3, respectively by summing the enthalpy of the exhaust gas leaving the combustor end and the heat loss through the quartz tube outer wall [4]. Thus, the estimated combustion efficiencies are 94.9 %, 90.3 %, and 90 % respectively for the G/M mixtures at the ratios of 50/ 50, 60/40, and 70/30 at an ALR of 3 and the constant theoretical HRR of 7 kW. In comparison, straight glycerol with extremely high viscosity was completely burned in the same 7 kW but insulated combustor owing to the fine FB atomization in our prior studies [4,12,22]. With further enhanced atomization, the SB injector integrating the FB injection concept [46,47] led to complete combustion of other straight oils including algae oil and vegetable oil [19,48] that are more viscous than the most viscous fuel blend (70/30 G/M) in the current study [4]. Therefore, the unburned fuel is (1) may be mainly due to the high ALR and thus high injection velocity resulting in some fuel leaving without sufficient residence time to be completely combusted; (2) and also possibly due to the high evaporation and auto-ignition temperatures of glycerol and the currently uninsulated combustor, which dissipates heat loss, reducing temperatures and thus fuel evaporation and oxidation rates in the combustor; and (3) some unburned larger droplets at the more viscous blends 60/40 and 70/30 compared to the G/M 50/50 case; (4) increased glycerol component in G/M 60/40, 70/30 than that of 50/ 50 [4]. Despite the more unburned fuels for the glycerol-denser fuel blends, the 50/50 G/M mix is near complete combustion at ALR of 3 owing to the effective SB atomization yet without fuel preheating nor insulation [4].

3.2. The effect of ALR on the global combustion characteristics

Previous studies have indicated that an increase in ALR results in finer atomization that might further benefit fuel evaporation, fuel–air mixing, and efficient combustion [4,46–48]. The present work also

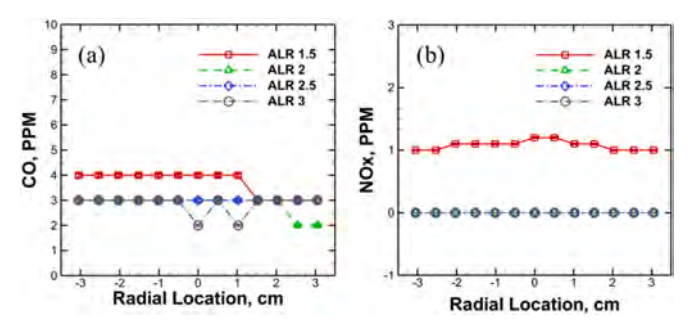


Fig. 8. Radial profiles of (a) CO and (b) NOx emissions for fuel mix G/M of 50/50 [4].

investigated the effect of ALR on the overall combustion characteristics of glycerol/methanol fuel blends, while keeping constant equivalence ratio, HRR and total air flow rate by varying the AA and PA flow rates [4]. The ALRs of 1.5, 2.0, 2.5, and 3.0 are employed to explore the combustion performance for the fuel blend 50/50 that is most comparable to diesel in terms of fuel properties [4] and G/M 70/30 that represents crude glycerol.

3.2.1. Global flame characteristics for 50/50 G/M

Fig. 7 displays the visual flame images of 50/50 at each of the four ALRs previously mentioned [4]. Each of the images show relatively similar flame structure with the visual flame beginning at the axial location of around y=10 cm and ending before y=25 cm [4]. As the ALR increases, flame width increases while flame length and flame lift-off slightly decrease [4]. This is possibly because of the finer droplets due to the increased ALR that evaporate faster and mix more homogenously with air, yielding a more radially distributed flame within the combustor at the highest ALR of 3.0 [4]. This also means that the

injector with higher AA can quickly break down larger particles at the higher ALR so that they can begin to combust sooner and in a shorter residence time than those at the lower ALRs, resulting in a slightly less limited flame at the high ALR though the droplet velocity is higher [4]. Despite the slight discrepancy, at all the ALRs, mainly lean-premixed flames are obtained indicative of the upstream dark region of fuel evaporation and mixing as the result of the fine SB atomization [4].

Fig. 8 shows the radial emissions profiles of CO and NOx at the combustor exit for the 50/50 fuel mixture at ALRs ranging from 1.5 to 3.0 [4]. The SB injector achieved ultra-low emissions at every ALR tested with CO < 5 ppm and NOx at nearly 0 [4]. With no nitrogen element in the fuel, NOx is mainly created by the thermal NOx mechanism that takes place at temperatures above 1800 K [4,19]. As shown in Fig. 9, the glycerol/methanol fuel mixtures did not reach temperatures near that mainly due to the high evaporation and auto-ignition temperature of the glycerol component and heat loss of the uninsulated combustor as aforementioned [4]. The 50/50 fuel mixture creates very low CO emissions which indicates near complete combustion for each ALR [4]. The CO emission readings are also ultra-low, even near the combustor walls indicating clean combustion possibly owing to the more uniform size distribution of droplets generated by the SB injector [4,46,47] compared to the FB injection and conventional atomizers such as airblast and pressure swirl injectors [4]. Decrease in ALR resulted in a slight increase in CO emissions, which is likely due to some slightly larger droplets burn locally at diffusion mode or incompletely. However, it is within the uncertainty range of CO measurement. Fig. 9 illustrates that the increase in ALR resulted in slightly lowered combustion exhaust gas temperature at the combustor exit [4]. This is possibly attributed to the increased injection velocity at the higher ALR that slightly shortens the residence time of the fuel blend in the combustor [4]. On the other hand, at the lower ALR, though the droplets might be slightly larger, fuel stayed longer in the combustor to further approach complete combustion and release more energy to raise up the gas product temperature

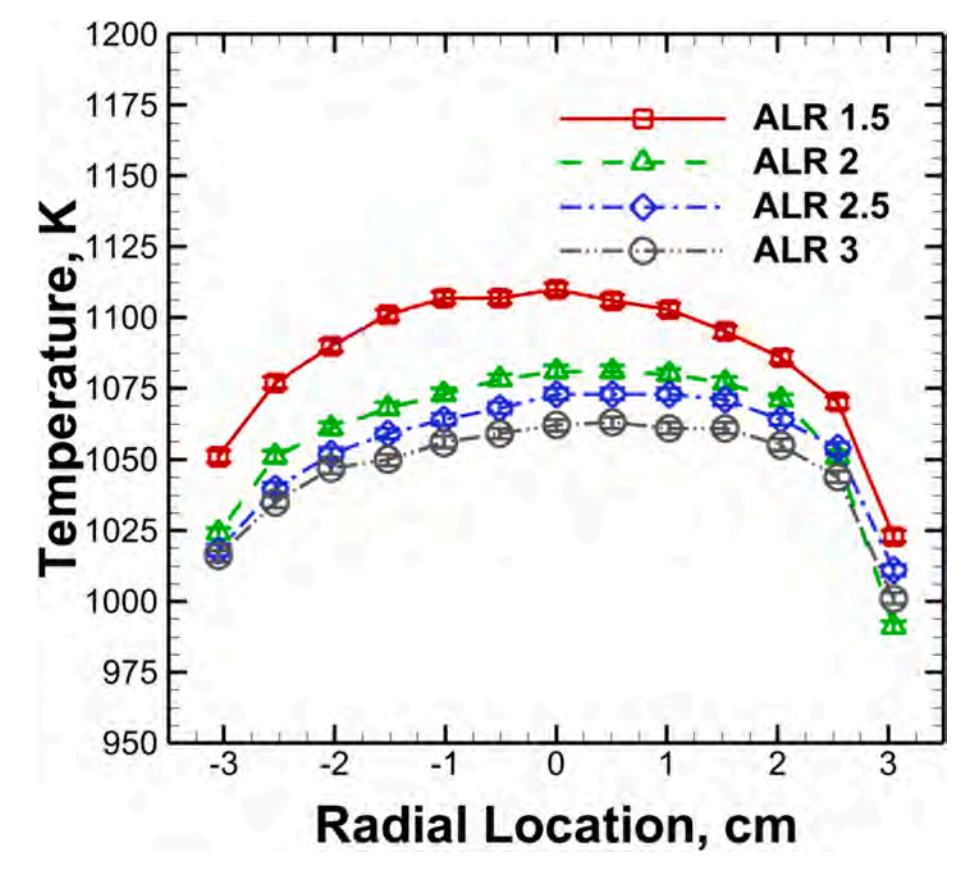


Fig. 9. Radial temperature profile of combustion products at the combustor exit at various ALRs for the G/M blend of 50/50 [4].

T. Hall et al. Fuel 371 (2024) 132125

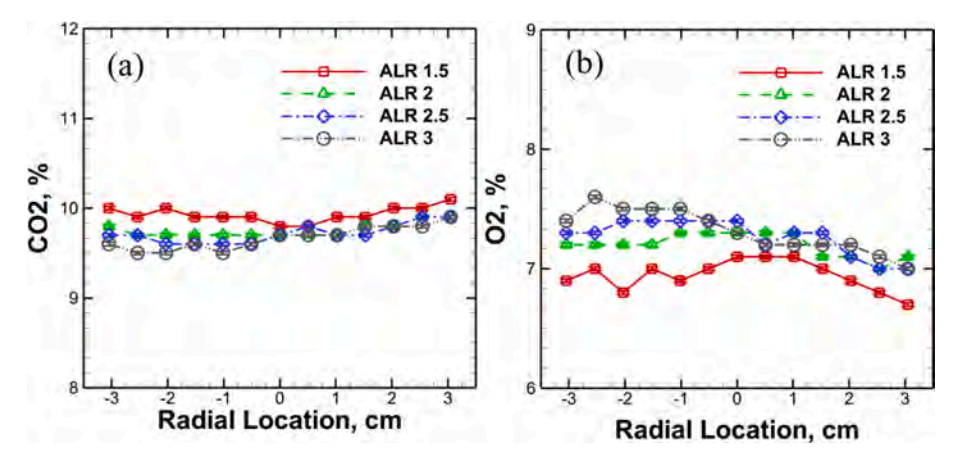


Fig. 10. Radial profiles of (a) CO₂ and (b) O₂ concentrations at the combustor exit for the G/M blend of 50/50 [4].

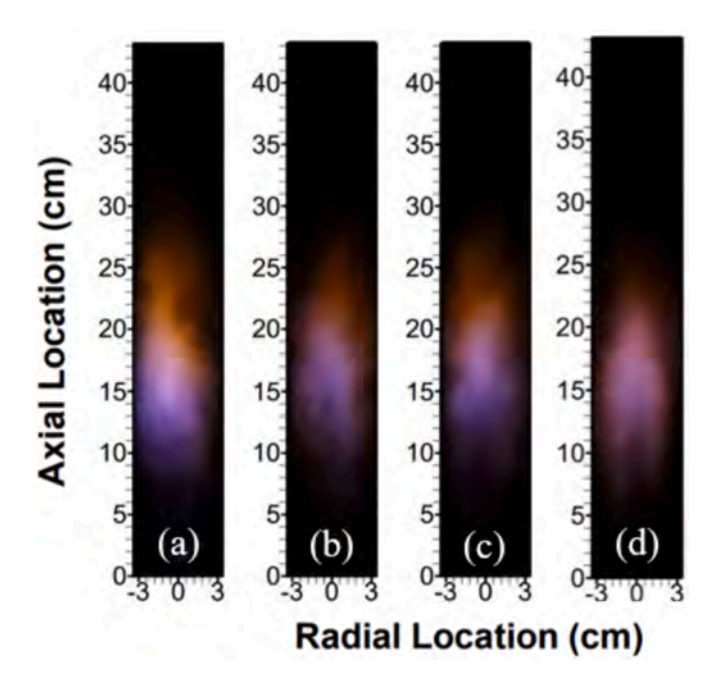


Fig. 11. Flame images for the glycerol/methanol (G/M) fuel mixture of 70/30 at ALRs of (a) 1.5 (b) 2.0 (c) 2.5 and (d) 3.0 at the constant HRR of 7 kW and equivalence ratio of 0.75.

[4]. Consistently, in Fig. 10, higher CO_2 and lower O_2 concentrations are measured at a lower ALR, again indicating more complete combustion at the lower ALR [4]. At ALR of 3, the previous estimate indicated near complete combustion for the 50/50 blend, signifying near complete combustion for all the tested ALRs owing to the fine SB atomization [4].

3.2.2. Global flame characteristics for 70/30 G/M

The effect of ALRs on the combustion characteristics of the 70/30 G/M by HRR is also investigated, which contains G/M ratio of 74.6/25.4 by weight and is also representative to crude glycerol from the transesterification process that contains $\sim\!62\text{--}76$ % glycerol [49] and $\sim\!23\text{--}38$ % methanol by weight [6]. The 70/30 G/M mix is $\sim\!4.5x$ viscous than conventional diesel as in Tables 1 and 2. Hence, it becomes difficult to combust effectively by conventional AB atomizer. Flame images of the ALRs of 1.5, 2.0, 2.5 and 3.0 for G/M 70/30 ratio by HRR are shown in Fig. 11. For all the ALRs, the dark region from the combustor dump plane to the upstream the flame suggests mainly LPM combustion. At the ALR of 1.5 more orange color reflects the soot chemiluminescence. With the increase in ALRs, probably due to

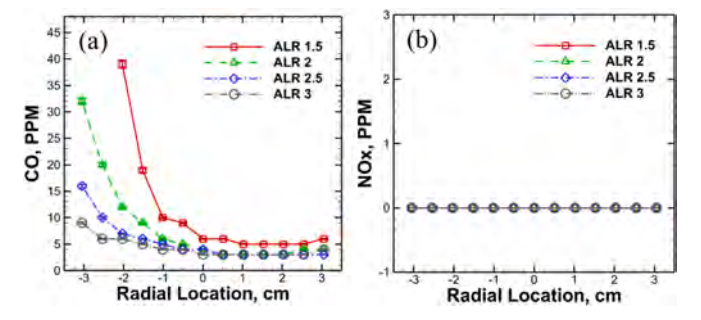


Fig. 12. Radial profiles of (a) CO and (b) NOx emissions for the fuel mix G/M of 70/30.

enhanced atomization, mainly blue flames were observed indicating clean combustion is achieved. Flames become more compact with the increase in ALR due to finer atomization that quickens fuel evaporation, mixing, and oxidation. At ALR of 1.5, the flame starts at around y = 8 cm and ends at y = 27 cm, with an approximate flame length of 19 cm. Whereas, at the higher ALR of 3.0, flame starts at y = 10 cm and ends at y = 23 cm, with a compact flame length of around 13 cm. It is also observed that the flames are slightly shifted to one side of the combustor. This may be attributed to (1) the turbulence nature of flame; (2) imperfect manufacturing of the SB injector that results in more larger droplets at one side than those on the other side [19]. More uniform distributed flame is observed at the increased ALR, which is likely due to finer droplets that rapidly and fully evaporate and result in homogenous fuel vapor-air mixture and thus combustion. Fig. 12 (a) and (b) exhibit the radial profiles of CO and NOx emissions at 1 in. upstream the combustor exit. It is seen that CO concentration of one side of the combustor is higher. In one side of the combustor, CO concentration is more than 100 ppm for ALR of 1.5, which is not shown in Fig. 12 (a). In consistent to the visual flame images, this is likely due to (1) more larger droplets at one side of the injector at the lower ALRs (1.5 and 2.0) which penetrate into the reaction zone without complete evaporation, resulting in less homogenous fuel air mixing in the near wall zone; (2) at the near wall zone, temperature is lower than the center zone of the combustor, which may lead to slower CO oxidation. Nevertheless, for ALR of 3.0, CO concentration is less than 10 ppm. This indicates that very fine and uniform size droplets are generated by the SB injector, which leads to rapid, complete evaporation with homogeneous fuel-air mixing. Thus, the novel SB injector achieved clean combustion even for a very high-viscosity G/M blend of 70/30 ratio, without fuel preheating.

Fig. 13 represents radial profiles of the exhaust gas temperature located at 1 in. upstream of the combustor exit. All the ALRs share similar temperature distribution. At the center of the combustor the

T. Hall et al. Fuel 371 (2024) 132125

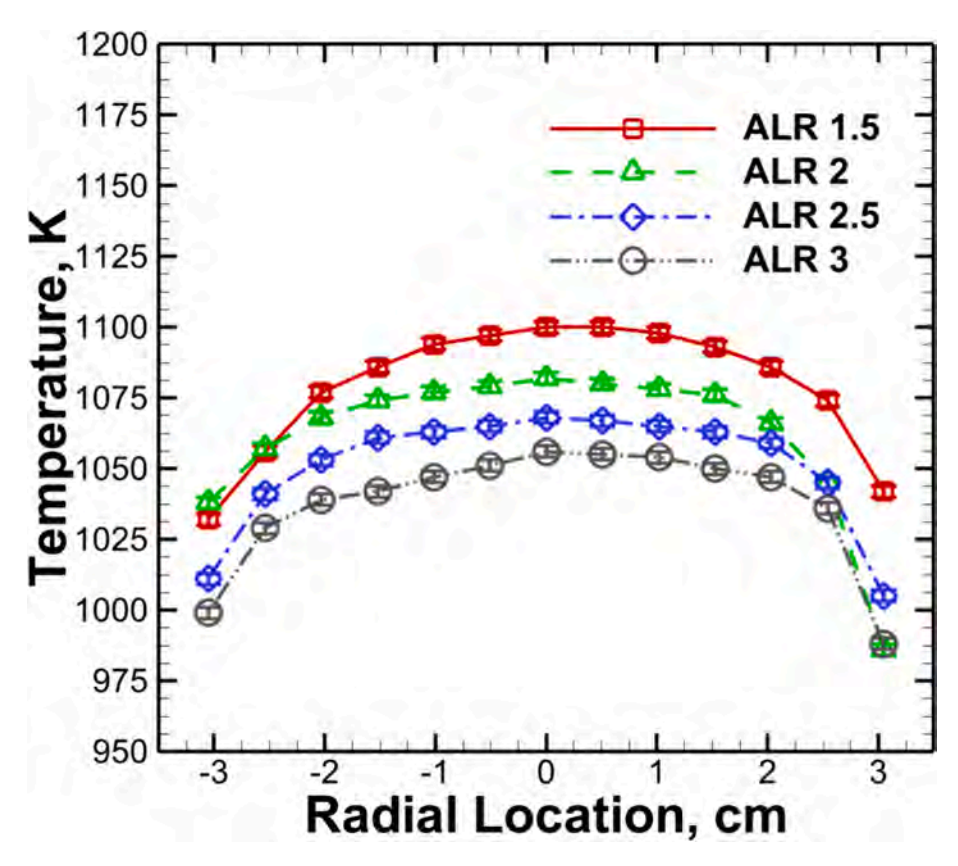


Fig. 13. Radial temperature profile of combustion products at the combustor exit at various ALRs for the G/M blend of 70/30.

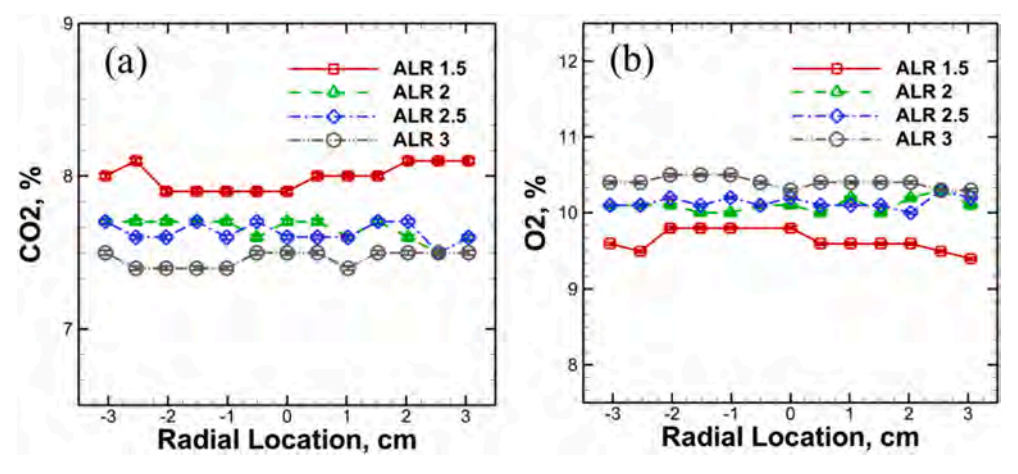


Fig. 14. Radial profiles of (a) CO₂ and (b) O₂ concentrations at the combustor exit for the G/M blend of 70/30.

temperature is higher compared to the near wall zone due to the heat loss through convection and radiation heat transfer in the near wall zone by the combustor quartz glass. Exhaust gas temperature is higher for lower ALRs. Again, this may be due to the lower ALR, injection velocity is lower at the decreased AA, which provides higher residence time to combust more completely. Besides, for the 70/30~G/M blend, the generated droplets may be slightly larger compared to the 50/50~and~60/40~G/M blends. These slightly larger droplets get more time to burn more completely and release more energy at lower ALRs when the injection velocity is reduced. For the lower ALR of 1.5, concentration of CO_2 is higher than that at the higher ALRs as per Fig. 14 (a), which consistently indicates that more complete combustion incurred for lower ALR of 1.5. Fig. 14 (b) illustrates O_2 concentration in exhaust gas, again substantiating that the completeness of combustion is higher for lower

ALRs, concentration of the remaining O_2 in exhaust gas is thus lower.

3.2.3. Combustion efficiency

Combustion completeness is estimated as aforementioned by summing the energy of the exhaust gas and the convection and radiation heat loss of the quartz combustor wall to the surrounding [19,50]. To minimize the thermocouple error, convection and radiation heat loss by the bead of thermocouple to the surrounding is taken into consideration and Eq. (2) is used to estimate the corrected exhaust gas temperature [19]. Estimated temperature difference between the thermocouple reading and true gas temperature is 346–402 K for ALR of 1.5–3.0 for 50/50 G/M and 334–391 K for ALRs of 1.5–3.0 for 70/30 G/M blends. To estimate total energy released by the combustion Eqs. (3)–(5) are used [19,45]. Theoretical input power is 7 kW. The estimated Cp of the

combustion exhaust gas are 1.4002, 1.3893, 1.3871 and 1.3834 for the ALRs of 1.5, 2.0, 2.5 and 3.0 for 50/50 G/M, based on the corrected gas temperature [43]. Similarly, the estimated Cp values are 1.3932, 1.3858, 1.3812 and 1.3753 for the ALRs of 1.5, 2.0, 2.5 and 3.0 for 70/30 G/M [43].

The estimated heat release for ALRs of 1.5, 2.0, 2.5 and 3.0 of G/M 50/50 blend are 6.97 kW, 6.81 kW, 6.61 kW and 6.64 kW respectively, signifying 99.5 %, 97.2 %, 94.5 % and 94.9 % combustion efficiency respectively. Our previous study found that an increase in ALR leads to a finer SB spray that is expected to evaporate faster for homogeneous fuelvapor and air mixing and thus clean and complete combustion [19,28]. It is interesting that with the increase in ALR, the combustion completeness degree decreases. This is attributed to the higher injection velocity at the higher ALR [4], at which the atomizing air flow rate is increased at the constant liquid flow. Hence, fuel residence time reduces, and fuel leaves the combustor without complete burn. This also signifies that the fine atomization already achieved at ALR of 1.5 by the SB injection. Also, this again substantiates that the incomplete combustion observed at ALR of 3 for the 50/50 G/M mix in the previous section 3.1 is due to the insufficient fuel residence time, rather than ineffective atomization, as increase in ALR further enhances atomization. From Fig. 10, it is also observed that at the lower ALR, CO₂ concentration in exhaust gas is higher and O2 concentration is lower compared to those at a higher ALR. This again substantiates that at a lower ALR, more fuel is burnt with higher O2 consumed and more CO2 generated and thus less excess O2 concentration in exhaust gas. Similar trend of completeness of combustion is observed for the different ALRs for 70/30 G/M blend. The estimated heat release rate for the ALRs of 1.5, 2.0, 2.5 and 3.0 of 70/30 G/M blend are 6.80 kW, 6.55 kW, 6.39 kW and 6.24 kW respectively, indicating the efficiency of 97.2 %, 93.6 %, 91.3 % and 90 % respectively. At the lower ALR of 1.5 for the least and most viscous blends of G/ M 50/50 and 70/30, the combustion is nearly completed despite of using uninsulated combustor and highly viscous fuel without pre-heating, reflecting the ultra-fine spray generation for the viscous mix by the SB injector. The viscosity range of the blends varied almost 5 times of diesel, which proves a very wide range of viscosity tolerance of the SB injector to combust fuel cleanly and efficiently with high fuel flexibility. Also, the SB injection at ALR of 1.5 results in complete combustion of all the G/M blends regardless of the distinct viscosity variations.

4. Conclusion

The current study investigates the combustion characteristics of glycerol/methanol blends using a novel twin-fluid injector with proved high-viscosity tolerance and fuel flexibility [4]. Biofuels, as oxygenated fuels, are highly desired to mitigate carbon footprint in energy generation [4]. The so-called SB injector utilizes a novel two-phase atomization concept to generate fine sprays immediately rather than a typical breaking jet/film of conventional atomizers such as air-blast or pressure swirl injectors widely used in gas turbine engines [4]. In the present study, the SB injection has yielded mainly lean-premixed combustion with ultra-low emissions of CO and NOx regardless of the wide range of fuel viscosity for the 50/50, 60/40, and 70/30 (~5x higher viscosity than diesel) of glycerol/methanol blends by percent HRR without fuel preheating nor insulation [4]. Estimate of energy released from the combustion indicates that the fuel blends of 50/50, 60/40, and 70/30 at an ALR of 3, achieve 94.9 %, 90.3 %, and 90 % complete combustion respectively [4]. The unburned fuel is mainly due to the high evaporation and auto-ignition temperature of the glycerol component in the uninsulated combustor [4]. For the fuel mix of 50/50 and 70/30, the increase in ALR results in more radially distributed flame and slightly reduced flame lift-off height due to the improved atomization at the higher ALR [4]. On the other hand, more complete combustion with higher product gas temperatures is acquired at lower ALRs due to lower injection velocity and thus longer residence time of fuels [4]. Estimated combustion completeness for ALRs of 1.5, 2.0, 2.5 and 3.0 of 50/50 G/M

blends are 99.5 %, 97.2 %, 94.5 % and 94.9 % respectively; and for ALRs of 1.5, 2.0, 2.5 and 3.0 of 70/30 G/M blends are 97.2 %, 93.6 %, 91.3 % and 90 % respectively. The SB injection at the ALR of 1.5 results in complete combustion for the least and most viscous G/M blends regardless of the distinct viscosity variations, showing its powerful atomization capability and high fuel flexibility for ultra-clean and efficient combustion. Each ALR achieves ultra clean and near-complete combustion with near zero emissions of CO and NOx [4]. Overall, the SB injection has enabled clean and near complete combustion of glycerol and methanol mixes representing crude glycerol with minimal waste processing without fuel preheating nor combustor insulation, signifying that the SB injector can enable the use of cost-effective biofuels for power generation with reduced carbon footprint [4].

CRediT authorship contribution statement

Timothy Hall: Writing – original draft, Methodology, Investigation, Formal analysis, Data curation. **Derek Williams:** Methodology, Investigation, Data curation. **S M Rafiul Islam:** Writing – original draft, Methodology, Formal analysis. **Ishaan Patel:** Methodology, Investigation, Data curation. **Caleb Chakmakjian:** Methodology, Data curation. **Lulin Jiang:** Writing – review & editing, Supervision, Resources, Project administration, Methodology, Funding acquisition, Formal analysis, Conceptualization.

Declaration of competing interest

The authors declare that they have no known competing financial interests or personal relationships that could have appeared to influence the work reported in this paper.

Data availability

Data will be made available on request.

Acknowledgments

The current research is funded by the Startup fund of Baylor University, NSF CIVIC award No. 2228311 by US National Science Foundation, and NSF CIVIC award No. 2322319 cofunded by US National Science Foundation and Department of Energy. We would also like to express our gratitude to Mr. Ashely Orr who helped manufacture the combustion system and Mr. Joseph Breerwood for helping set up the system.

References

- [1] Pasha MK, Dai L, Liu D, Guo M, Du W. An overview to process design, simulation and sustainability evaluation of biodiesel production. Biotechnol Biofuels 2021;14: 129. https://doi.org/10.1186/s13068-021-01977-z.
- [2] UFOP. Report on Global Market Supply: 2019/2020, Berlin, 2020. 2020. https://library.wur.nl/WebQuery/titel/2289027 (accessed February 7, 2024).
- [3] Farag HA, El-Maghraby A, Taha NA. Transesterification of esterified mixed oil for biodiesel production; 2012.
- [4] Jiang L, Hall T, Williams D, Swinney R. Global Combustion Characteristics of Glycerol and Methanol Blends Using a Novel Fuel-Flexible Injector. In: AIAA SCITECH 2023 Forum. National Harbor, MD & Online: American Institute of Aeronautics and Astronautics; 2023. https://doi.org/10.2514/6.2023-0495.
- [5] Leung DYC, Wu X, Leung MKH. A review on biodiesel production using catalyzed transesterification. Appl Energy 2010;87:1083–95. https://doi.org/10.1016/j. appnergy.2009.10.006.
- [6] Quispe CAG, Coronado CJR, Carvalho Jr JA. Glycerol: Production, consumption, prices, characterization and new trends in combustion. Renew Sustain Energy Rev 2013;27:475–93. https://doi.org/10.1016/j.rser.2013.06.017.
- [7] Agwu O, Valera-Medina A, Katrašnik T, Seljak T. Flame characteristics of glycerol/methanol blends in a swirl-stabilised gas turbine burner. Fuel 2021;290:119968. https://doi.org/10.1016/j.fuel.2020.119968.
- [8] Okoye PU, Abdullah AZ, Hameed BH. Synthesis of oxygenated fuel additives via glycerol esterification with acetic acid over bio-derived carbon catalyst. Fuel 2017; 209:538–44. https://doi.org/10.1016/j.fuel.2017.08.024.

- [9] Spataru D, Soares Dias AP, Vieira Ferreira LF. Acetylation of biodiesel glycerin using glycerin and glucose derived catalysts. J Clean Prod 2021;297:126686. https://doi.org/10.1016/j.jclepro.2021.126686.
- [10] Jiang L, Agrawal AK. Combustion of straight glycerol with/without methane using a fuel-flexible, low-emissions burner. Fuel 2014;136:177–84. https://doi.org/ 10.1016/j.fuel.2014.07.027.
- [11] Zhang J, Wang Y, Muldoon VL, Deng S. Crude glycerol and glycerol as fuels and fuel additives in combustion applications. Renew Sustain Energy Rev 2022;159: 112206. https://doi.org/10.1016/j.rser.2022.112206.
- [12] Ferreira AGM, Egas APV, Fonseca IMA, Costa AC, Abreu DC, Lobo LQ. The viscosity of glycerol. J Chem Thermodyn 2017;113:162–82. https://doi.org/10.1016/j. iet.2017.05.042
- [13] Seljak T, Katrašnik T. Emission reduction through highly oxygenated viscous biofuels: use of glycerol in a micro gas turbine. Energy 2019;169:1000–11. https://doi.org/10.1016/j.energy.2018.12.095.
- [14] Pillai AL, Nagao J, Awane R, Kurose R. Influences of liquid fuel atomization and flow rate fluctuations on spray combustion instabilities in a backward-facing step combustor. Combust Flame 2020;220:337–56. https://doi.org/10.1016/j. combustflame.2020.06.031.
- [15] Simmons BM, Panchasara HV, Agrawal AK. A Comparison of Air-Blast and Flow-Blurring Injectors Using Phase Doppler Particle Analyzer Technique. Volume 2: Combustion, Fuels and Emissions, Orlando, Florida, USA: ASMEDC; 2009, p. 981–92. https://doi.org/10.1115/GT2009-60239.
- [16] Zhang T, Dong B, Chen X, Qiu Z, Jiang R, Li W. Spray characteristics of pressureswirl nozzles at different nozzle diameters. Appl Therm Eng 2017;121:984–91. https://doi.org/10.1016/j.applthermaleng.2017.04.089.
- [17] Hendershott TH, Stouffer S, Monfort JR, Diemer J, Busby K, Corporan E, et al. Ignition of Conventional and Alternative Fuel at Low Temperatures in a Single-Cup Swirl-Stabilized Combustor. In: 2018 AIAA Aerospace Sciences Meeting. Kissimmee, Florida: American Institute of Aeronautics and Astronautics; 2018. https://doi.org/10.2514/6.2018-1422.
- [18] Gañán-Calvo AM. Enhanced liquid atomization: From flow-focusing to flow-blurring. Appl Phys Lett 2005;86:214101. https://doi.org/10.1063/1.1931057.
- [19] Akinyemi OS, Jiang L. Development and combustion characterization of a novel twin-fluid fuel injector in a swirl-stabilized gas turbine burner operating on straight vegetable oil. Exp Therm Fluid Sci 2019;102:279–90. https://doi.org/10.1016/j. exothermflusci.2018.11.014.
- [20] Akinyemi OS, Jiang L, Hernandez R, McIntyre C, Holmes W. Combustion of straight algae oil in a swirl-stabilized burner using a novel twin-fluid injector. Fuel 2019;241:176–87. https://doi.org/10.1016/j.fuel.2018.12.006.
 [21] Qavi I, Jiang L, Akinyemi OS. Near-field spray characterization of a high-viscosity
- [21] Qavi I, Jiang L, Akinyemi OS. Near-field spray characterization of a high-viscosity alternative jet fuel blend C-3 using a flow blurring injector. Fuel 2021;293:120350. https://doi.org/10.1016/j.fuel.2021.120350.
- [22] Jiang L, Agrawal AK. Investigation of glycerol atomization in the near-field of a flow-blurring injector using time-resolved PIV and high-speed visualization. Flow Turbulence Combust 2015;94:323–38. https://doi.org/10.1007/s10494-014-9572-2.
- [23] Simmons BM, Agrawal AK. Flow blurring atomization for low-emission combustion of liquid biofuels. Combust Sci Technol 2012;184:660–75. https://doi.org/ 10.1080/00102202.2012.660222.
- [24] Jiang L, Agrawal AK, Taylor RP. Clean combustion of different liquid fuels using a novel injector. Exp Therm Fluid Sci 2014;57:275–84. https://doi.org/10.1016/j. expthermflusci 2014 05 002
- [25] Panchasara HV, Sequera DE, Schreiber WC, Agrawal AK. Emissions reductions in diesel and kerosene flames using a novel fuel injector. J Propul Power 2009;25: 984–7. https://doi.org/10.2514/1.37165.
- [26] Jiang L, Agrawal AK. Spray features in the near field of a flow-blurring injector investigated by high-speed visualization and time-resolved PIV. Exp Fluids 2015; 56:103. https://doi.org/10.1007/s00348-015-1973-z.
- [27] Danh V, Jiang L, Akinyemi OS. Investigation of water spray characteristics in the near field of a novel swirl burst injector. Exp Therm Fluid Sci 2019;102:376–86. https://doi.org/10.1016/j.expthermflusci.2018.12.014.
- [28] Danh V, Akinyemi OS, Taylor CE, Frank JT, Jiang L. Effect of injector swirl number on near-field spray characteristics of a novel twin-fluid injector. Exp Fluids 2019; 60:80. https://doi.org/10.1007/s00348-019-2721-6.

- [29] Qavi I, Jiang L. Optical characterization of near-field sprays for various alternative and conventional jet fuels using a flow-blurring injector. Flow Turbulence Combust 2022;108:599–624. https://doi.org/10.1007/s10494-021-00276-9.
- [30] Chilakamarry CR, Mimi Sakinah AM, Zularisam AW, Pandey A, Vo D-V-N. Technological perspectives for utilisation of waste glycerol for the production of biofuels: a review. Environ Technol Innov 2021;24:101902. https://doi.org/ 10.1016/j.eit.2021.101902.
- [31] He Q (Sophia), McNutt J, Yang J. Utilization of the residual glycerol from biodiesel production for renewable energy generation. Renew Sustain Energy Rev 2017;71: 63–76. https://doi.org/10.1016/j.rser.2016.12.110.
- [32] Deka TJ, Osman AI, Baruah DC, Rooney DW. Methanol fuel production, utilization, and techno-economy: a review. Environ Chem Lett 2022;20:3525–54. https://doi. org/10.1007/s10311-022-01485-y
- [33] Marulanda VF. Biodiesel production by supercritical methanol transesterification: process simulation and potential environmental impact assessment. J Clean Prod 2012;33:109–16. https://doi.org/10.1016/j.jclepro.2012.04.022.
- [34] Gülüm M, Bilgin A. A comprehensive study on measurement and prediction of viscosity of biodiesel-diesel-alcohol ternary blends. Energy 2018;148:341–61. https://doi.org/10.1016/j.energy.2018.01.123.
- [35] Jin C, Sun T, Xu T, Jiang X, Wang M, Zhang Z, et al. Influence of glycerol on methanol fuel characteristics and engine combustion performance. Energies 2022; 15:6585. https://doi.org/10.3390/en15186585.
- [36] De Oliveira GS, Lobo CES, Padilha CEA, Souza DFS, Ruiz JAC. Glycerin combustion through chemical looping. Fuel 2023;352:129038. https://doi.org/10.1016/j. fuel 2023 129038
- [37] Lilley DG. Swirl flows in combustion: a review. AIAA J 1977;15:1063–78. https://doi.org/10.2514/3.60756.
- [38] Duraisamy G, Rangasamy M, Govindan N. A comparative study on methanol/diesel and methanol/PODE dual fuel RCCI combustion in an automotive diesel engine. Renew Energy 2020;145:542–56. https://doi.org/10.1016/j.renene.2019.06.044.
- [39] Li Z, Wang Y, Geng H, Zhen X, Liu M, Xu S, et al. Effects of diesel and methanol injection timing on combustion, performance, and emissions of a diesel engine fueled with directly injected methanol and pilot diesel. Appl Therm Eng 2019;163: 114234. https://doi.org/10.1016/j.applthermaleng.2019.114234.
- [40] Wang Y, Wang H, Meng X, Tian J, Wang Y, Long W, et al. Combustion characteristics of high pressure direct-injected methanol ignited by diesel in a constant volume combustion chamber. Fuel 2019;254:115598. https://doi.org/ 10.1016/j.fuel.2019.06.006.
- [41] Turns SR. An introduction to combustion: concepts and applications. 3rd ed. New York: McGraw-Hill; 2012.
- [42] Çengel YA, Ghajar AJ. Heat and mass transfer: fundamentals & applications. 5th ed. New York, NY: McGraw Hill Education; 2015.
- [43] Çengel YA, Boles MA. Thermodynamics: an engineering approach. 8th ed. New York: McGraw-Hill Education: 2015.
- [44] Petrov V, Reznik V. Measurement of the emissivity of quartz glass. High Temperatures-High Pressures 1972;4:687–93.
- [45] Çengel YA. Heat Transfer: A Practical Approach. Second Edition. McGraw-Hill Companies; 2002.
- [46] Lefebvre AH. Airblast atomization. Prog Energy Combust Sci 1980;6:233–61. https://doi.org/10.1016/0360-1285(80)90017-9.
- [47] Simmons BM, Agrawal AK. Spray characteristics of a flow-blurring atomizer. Atomiz Spr 2010;20:821–35. https://doi.org/10.1615/AtomizSpr.v20.i9.60.
- [48] Institute of Mechanics and Thermodynamics, Chemnitz University of Technology, Chemnitz, Germany, Roudini M, Wozniak G. Investigation of the Secondary Atomization in Prefilming Air-Blast Atomizers. IJCEA 2019;10:138–43. https://doi.org/10.18178/ijcea.2019.10.5.757.
- [49] Thompson JC, He BB. Characterization of crude glycerol from biodiesel production from multiple feedstocks. Appl Eng Agric 2006;22:261–5. https://doi.org/ 10.13031/2013.20272.
- [50] Shannon KS, Butler BW. A review of error associated with thermocouple temperature measurement in fire environments. In: 2nd International Wildland Fire Ecology and Fire Management Congress and the 5th Symposium on Fire and Forest Meteorology; 2003.